



Peroxidative bromination and oxygenation of organic compounds: Synthesis, X-ray crystal structure and catalytic implications of mononuclear and binuclear oxovanadium(V) complexes containing Schiffbase ligands

Tapan Kumar Si^{a,*}, Michael G.B. Drew^b, Kalyan Kumar Mukherjea^{a,*}

^a Department of Chemistry, Jadavpur University, Kolkata 700032, India

^b Department of Chemistry, The University of Reading, P.O. Box 224, Whiteknights, Reading RG6 6AD, UK

ARTICLE INFO

Article history:

Received 12 May 2011

Accepted 12 June 2011

Available online 25 June 2011

Keywords:

Oxovanadium(V) Schiffbase complex

Crystal structure

Catalytic oxidation

Haloperoxidase activity

Hydrogen peroxide

ABSTRACT

Treatment of of (*R,R*)-*N,N*-salicylidene cyclohexane 1,2-diamine(H_2L^1) in methanol with aqueous NH_4VO_3 solution in perchloric acid medium affords the mononuclear oxovanadium(V) complex $[VOL^1(MeOH)] \cdot ClO_4$ (**1**) as deep blue solid while the treatment of same solution of (*R,R*)-*N,N*-salicylidene cyclohexane 1,2-diamine(H_2L^1) with aqueous solution of $VOSO_4$ leads to the formation of di-(μ -oxo) bridged vanadium(V) complex $[VO_2L^2]_2$ (**2**) as green solid where $HL^2 = (R,R)$ -*N*-salicylidene cyclohexane 1,2-diamine. The ligand HL^2 is generated in situ by the hydrolysis of one of the imine bonds of HL^1 ligand during the course of formation of complex $[VO_2L^2]_2$ (**2**). Both the compounds have been characterized by single crystal X-ray diffraction as well as spectroscopic methods. Compounds **1** and **2** are to act as catalyst for the catalytic bromide oxidation and C–H bond oxidation in presence of hydrogen peroxide. The representative substrates 2,4-dimethoxy benzoic acid and para-hydroxy benzoic acids are brominated in presence of H_2O_2 and KBr in acid medium using the above compounds as catalyst. The complexes are also used as catalyst for C–H bond activation of the representative hydrocarbons toluene, ethylbenzene and cyclohexane where hydrogen peroxide acts as terminal oxidant. The yield percentage and turnover number are also quite good for the above catalytic reaction. The oxidized products of hydrocarbons have been characterized by GC Analysis while the brominated products have been characterized by 1H NMR spectroscopic studies.

© 2011 Elsevier Ltd. All rights reserved.

1. Introduction

Research in oxovanadium chemistry containing the vanadium–oxygen core moieties VO_2^+ , VO^{3+} and VO^{2+} has gained a special momentum in the field of homogeneous catalytic research as they involve the conversion of crude oil and natural gas constituents into their oxygenated derivatives in presence of hydrogen peroxide [1,2]. The discovery [3] of the core species present in the active site (VO_4N) of the enzymes of biological systems in the form of vanadium-dependent haloperoxidases (VHPO) [4–7] and insulin mimicking behavior of oxovanadium compounds have also increased the importance in the field of research of oxovanadium chemistry. The haloperoxidases are known to function as essential enzymes for the biosynthesis of halogenated natural products [8] catalyzing the oxidation of halides [9,10] by hydrogen peroxide to corresponding HOX , X_3^- or X_2 (X = halogen). The vanadium(V) complexes have also been found to act as catalyst precursors in various oxidation

reactions e.g. epoxidation of alkenes and allylic alcohols [11–15], oxygenation of alkanes, arenes and primary or secondary alcohols to the corresponding aldehydes or ketones [16–19] as well as oxidation of organic sulfides [20–22] to sulfoxides and sulfones in presence of hydrogen peroxide. It may be noted that the tridentate and tetradentate Schiffbase complexes of vanadium are well established [23] but the report of these complexes that are used as catalyst for hydrocarbon oxidation and halides oxidation are still very scanty [24]. Mohebbi and Sererstini [25] reported a good yield with improved turnover number (TON) (integrated) for olefin epoxidation using VO-tetradentate Schiffbase complexes as catalyst and O_2 as an oxidant in CH_3CN medium where the conversion of the substrates were dependent on the nature of substituent in the Schiffbase ligand. The oxovanadium(V) complexes with (*R,R*)-*N,N*-salicylidene cyclohexane 1,2-diamine was first reported by Nakajima et al. [26] and later by some other groups [27,28] but none of them examined their multifunctional catalytic activity. Herein, we are reporting the synthesis and structural characterization of a new mononuclear complex of oxovanadium(V) $[VOL^1(MeOH)] \cdot ClO_4$ (**1**) of tetradentate Schiffbase ligand (*R,R*)-*N,N*-di-salicylidene cyclohexane 1,2-diamine(H_2L^1) and a di-(μ -oxo) bridged vanadium(V) complex $[VO_2L^2]_2$

* Corresponding authors. Tel./fax: +91 33 24146223.

E-mail addresses: tksi2002@yahoo.co.in (T.K. Si), k_mukherjea@yahoo.com (K.K. Mukherjea).

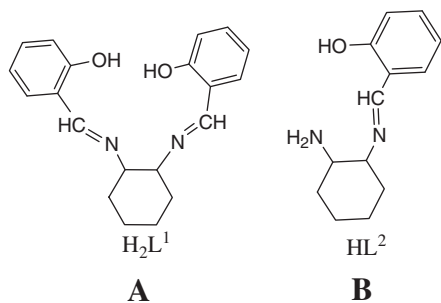


Fig. 1. Ligand: H_2L^1 = (*R,R*)-*N,N*-di-salicylidene cyclohexane 1,2-diamine(A) and HL^2 = (*R,R*)-*N*-salicylidene cyclohexane 1,2-diamine (B).

(**2**) of tridentate Schiffbase (*R,R*)-*N*-salicylidene cyclohexane 1,2-diamine(HL^2). Though the structural characterization of compound **2** has appeared in a recent literature [29] in 2009, but herein, the same compound is being reported with different synthesis procedure along with the catalytic implications of both the compounds **1** and **2** towards C–H bond oxidation as well as bromide oxidation with good yield percentage and turnover number for such oxidation reactions. The structure of the chiral Schiffbase ligands is represented in Fig. 1.

2. Experimental

2.1. Materials and methods

Ammonium metavanadate, cyclohexane, cyclohexanol and cyclohexanone were of extrapure variety and obtained from Sisco Research Laboratory (India). Salicylaldehyde and Vanadyl Sulfate were obtained from S.D. Fine-Chem. Ltd. (India) and *trans*-1,2-cyclohexanediamine was obtained from Aldrich Chemical Co., Ltd. Potassium bromide and methanol (G.R.) were the products of E. Merck (India) and were directly used. Ethanol (95%) was obtained from Bengal Chemical and Pharmaceutical Works (Calcutta), and was lime distilled before use. All other chemicals needed were obtained from E. Merck (India). Acetonitrile, dichloromethane and acetone were further purified by literature method for physico-chemical studies. Iolar II grade dioxygen, dihydrogen, zero air, and dinitrogen gas used for chromatographic analysis were obtained from Indian Refrigeration Stores, Calcutta. Triply distilled (all glass) water was used whenever necessary. All the solvents used for chromatographic analysis were either of HPLC, spectroscopic, or GR grade and in all cases their purity was confirmed by GC analysis before use. The IR spectra were recorded as KBr pellets on a Perkin–Elmer 597 IR spectrophotometer (4000–200 cm^{-1}) and Electronic spectra on a Hitachi U-3410 UV/Vis–NIR spectrophotometer. 1H NMR spectra were measured in $CDCl_3$ on a Bruker AM 360 (300 MHz) FT NMR spectrometer using TMS as an internal standard. A systronics (India) model 335 digital conductivity bridge with a bottle type cell was used to determine the molar conductance values of the isolated complexes at 25 °C using a thermostatic arrangement. A SUNVIC (UK) apparatus was used to measure melting point of the organic substrates as well as their oxidized products. Elemental analyses were performed with the help of a Perkin–Elmer 240C elemental analyzer. GLC measurements were done in an Agilent model 6890 gas chromatograph using HP-1 and INNOWAX capillary column in FID mode with dinitrogen as carrier gas.

2.2. Synthesis of ligand (H_2L^1)

The ligand *N,N*-bis(salicylidene)cyclohexane 1,2-diamine (H_2L^1) was prepared by refluxing the mixture of salicylaldehyde (20 mmol)

and *trans*-1,2-cyclohexanediamine (10 mmol) in 25 ml dry methanol for 5–6 h. Then yellow crystalline precipitate of H_2L^1 was deposited. The solid mass was collected and dried in vacuo. Yield 2.80 g (85%). *Anal. Calc.* for $C_{20}H_{20}N_2O_2$: C, 74.96; H, 6.29; N, 8.74. Found: C, 74.83; H, 6.21; N, 8.96%. IR (KBr disc, cm^{-1}): 3481(b)[O–H], 2921(w), 2850(w), 1629(s)[C=N], 1581(w), 1500(m), 1461(w), 1421(w), 1382(w), 1340(w), 1280(s), 1215(w), 1147(m), 1095(w), 1043(w), 939(w), 846(m), 763(s), 667(w), 655(w), 364(w). The *trans*-1-salicylideneimine 2-amine-cyclohexane (HL^2) was prepared in situ by the reaction of H_2L^1 ligand (2 mmol) in 10 ml methanol with $VOSO_4 \cdot H_2O$, (2 mmol) with constant stirring.

2.3. Synthesis of $[VO(L^1)(CH_3OH)] \cdot ClO_4$ (**1**)

$VOSO_4 \cdot H_2O$, 0.186 g (1 mmol) was dissolved in aqueous medium and acidified by perchloric acid followed by addition of methanolic solution of H_2L^1 , 0.323 g (1 mmol) with constant stirring. A deep blue colored compound precipitated. Solid products was collected through filtration and dried in vacuo after washing it by diluted methanol. Yield 0.268 g (52%). *Anal. Calc.* for $C_{21}H_{23}ClN_2O_8V$: V, 9.85; C, 48.69; H, 4.44; N, 5.41. Found: V, 9.71; C, 48.33; H, 4.21; N, 5.75%. IR(KBr disc, cm^{-1}): 3448(b), 2943(w), 2864(w), 2367(w), 2340(w), 1613(s)[C=N], 1553(s), 1447(s), 1390(m), 1345(w), 1305(s), 1274(s), 1228(w), 1114(s), 1073(s), 974(s)[V=O], 911(m), 864(w), 828(s), 766(s), 661(s), 625(m), 581(m), 552(w), 509(m), 481(w), 454(m). UV–Vis; λ_{max} nm (ϵ $M^{-1} cm^{-1}$): 567(1800), 466(sh), 249 (27,100), 235(sh).

2.4. Synthesis of $[V_2O_4(L^2)_2]$ (**2**)

Dissolved the ligand H_2L^1 , 0.323 g (1 mmol) in 10 ml methanol and then it was added to the methanolic solution of $VOSO_4 \cdot H_2O$, 0.167 g (1 mmol) with constant stirring. Immediately a deep glass-green color complex of $V_2O_4(L^2)_2$, **2** was obtained. The complex **2** is insoluble in water, methanol, ethanol, acetonitrile or other highly polar solvents but soluble in dichloromethane and chloroform slowly. Yield 0.33 g (55%). *Anal. Calc.* for $C_{26}H_{34}N_4O_6V_2$: V, 17.00; C, 52.00; H, 5.66; N, 9.33. Found: V, 16.51; C, 51.33; H, 5.85; N, 9.54%. IR (KBr disc, cm^{-1}): 3448(b), 3052(w), 2933(m), 2860(w), 2367(w), 2340(w), 1614(s)[C=N], 1543(s), 1447(s), 1392(m), 1347(w), 1311(s)[C–O_{enolate}], 1200(m), 1147(m), 1093(w), 1064(w), 979(s)[V=O], 908(m), 858(w), 810(m), 760(s), 680(w), 621(s), 570(w), 492(w), 424(w). UV–Vis; λ_{max} nm (ϵ $M^{-1} cm^{-1}$): 592(5300), 366(sh), 280(99,100), 267(sh).

2.5. X-ray crystallography

The good quality deep blue crystals of **1** were obtained by slow diffusion of petroleum ether into acetone solution of the compound **1** while glass-green crystals of **2** were obtained by slow evaporation of chloroform solution of compound **2**. The crystals were very narrow needles and diffracted weakly. X-ray intensity data were measured at 150 K using the Oxford X-Calibur CCD System [30], with Mo $K\alpha$ radiation. The crystals were positioned at 50 mm from the CCD. 321 frames were measured with a counting time of 3 s. The structures were solved using direct methods with the program SHELXS and refined using the program SHELXL [31]. The non-hydrogen atoms were refined with anisotropic thermal parameters. The hydrogen atoms bonded to carbon were included in geometric positions and given thermal parameters equivalent to 1.2 times those of the atom to which they were attached. Empirical absorption corrections were carried out using the ABSPACK program [32]. The structures were refined on F^2 using SHELXL. Crystal data, structure solution and refinement parameters for complexes **1** and **2** are summarized in Table 1.

Table 1
Crystal data and structure refinement parameters for complexes **1** and **2**.

	1	2
Empirical formula	C ₂₁ H ₂₃ ClN ₂ O ₈ V	C ₂₆ H ₃₄ N ₄ O ₆ V ₂
Molecular weight	517.18	600.46
T (K)	153(2)	153(2)
λ (Å)	0.71073	0.71073
Crystal system	triclinic	monoclinic
Space group	<i>P</i> $\bar{1}$	<i>P</i> 2 ₁ / <i>a</i>
Unit cell dimensions		
<i>a</i> (Å)	9.367(3)	8.8637(8)
<i>b</i> (Å)	11.316(3)	12.4952(18)
<i>c</i> (Å)	11.690(4)	11.8915(13)
α (°)	108.61(3)	–
β (°)	107.92(3)	103.73(1)
γ (°)	90.23(3)	–
<i>V</i> (Å ³), <i>Z</i>	1110.2(6), 2	1279.4(3), 2
<i>D</i> _{calc} (g cm ^{−3})	1.549	1.559
<i>F</i> (0 0 0)	534	624
Crystal size (mm)	0.03 × 0.03 × 0.22	0.02 × 0.04 × 0.27
θ Range for data collection (°)	2.30–30.00	2.90–30.10
Reflections collected	9641	7008
Independent reflections (<i>R</i> _{int})	6106(0.040)	3626(0.077)
Completeness to $\theta = \theta_{\max}$ (%)	94.4	95.8
Refinement method	full-matrix-least-squares on <i>F</i> ²	
Absorption correction (<i>T</i> _{min} , <i>T</i> _{max})	0.783, 1.243	0.761, 1.293
Data/restraints/parameters	6106/0/298	3626/0/172
Goodness-of-fit (GOF) on <i>F</i> ²	0.638	0.995
Final <i>R</i> indices [<i>I</i> > 2 σ (<i>I</i>)]	<i>R</i> ₁ = 0.0487 <i>wR</i> ₂ = 0.1046	<i>R</i> ₁ = 0.0988 <i>wR</i> ₂ = 0.2498
<i>R</i> indices (all data)	<i>R</i> ₁ = 0.1518 <i>wR</i> ₂ = 0.1114	<i>R</i> ₁ = 0.1529 <i>wR</i> ₂ = 0.2771
Largest differences in peak and hole (e Å ^{−3})	1.458, −1.206	1.554, −1.337


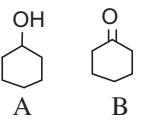
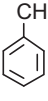
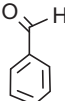
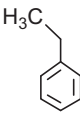
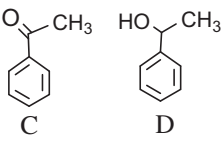
2.6. Experimental setup of catalytic bromination

Catalyst and substrate (substituted benzoic acid) with a mole ratio (1:1000) was dissolved in 5 ml CH₃CN and then 3 ml aqueous solution of KBr, 1.18 g (10 mmol) was added followed by the addition of 2.5 ml 30% of H₂O₂ with constant stirring at room temperature. 1(N) nitric acid was added for maintaining the medium acidic (pH 3). After 12 h the reaction was stopped and collected the organic part with ether extract. After evaporation solid product was isolated and studied by the ¹H NMR spectroscopy for analysis of the catalytic products.

2.7. Experimental setup of catalytic oxidation of hydrocarbons

An acetonitrile solution (10 cm³) containing a given substrate (5 mmol), oxovanadium(V) catalyst (0.05–0.005 mmol) and 30%

Table 2
Details of catalytic hydrocarbon oxidation by compound **1** and **2** used as catalyst in presence of H₂O₂ and CH₃CN as solvent.

Entry	Substrate	Product (s)	Time (h)	% Yields (mmol) for catalyst		% Selectivity/proportion for catalyst		Turn over number (TON)	
				1	2	1	2	1	2
1		 A B	10	100	78	A-30 B-70	A-40 B-60	990	780
2			20	43	24	100	100	430	120
3		 C D	20	60	47	C-96 D-4	C-95 D-5	600	470

H₂O₂ (20 mmol) in a high-pressure reactor (100 mL capacity Parr type hydrogenation apparatus) at 60–80 °C was stirred for definite period as presented in Table 2. When required, an aliquot of the reaction solution was withdrawn with the help of long needle syringe and was subjected to multiple ether extractions and 1 μ L of concentrated ether extract was injected to the GC port with the help of 10 μ L syringe. The retention times of the peaks were compared with those of commercial standards and the unknown peaks were characterized by GC–MS analysis. Parr type apparatus was used for the convenience of the physico-chemical studies but it is not absolutely necessary for laboratory as well as industry.

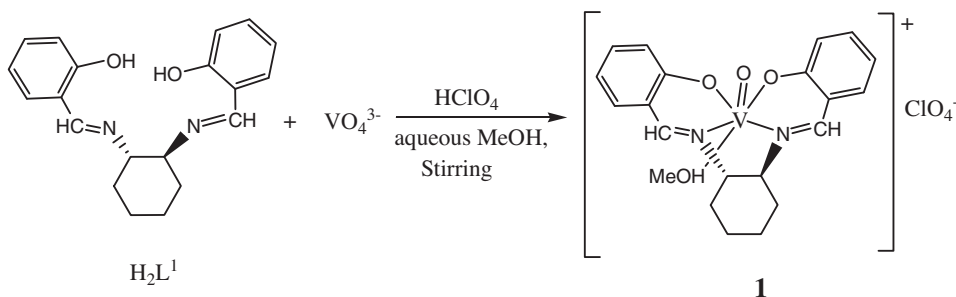
3. Results and discussion

3.1. Synthetic aspects

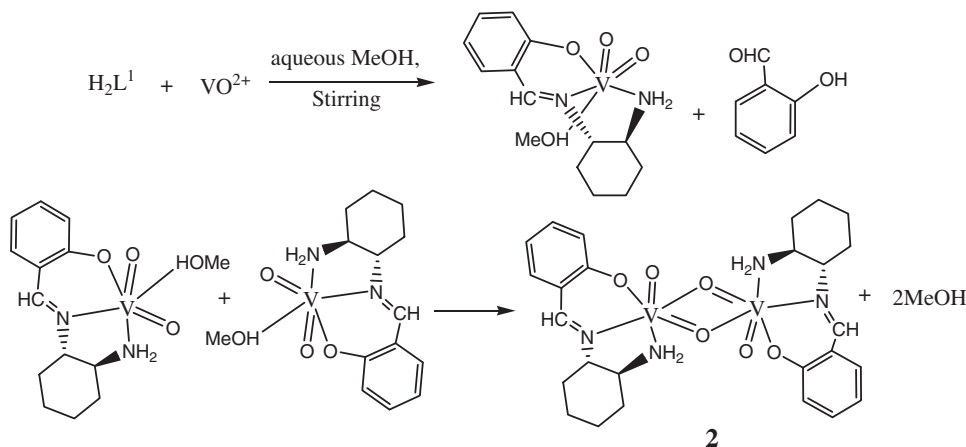
H₂L¹ reacts with NH₄VO₃ solution acidified with perchloric acid yielding [VO(L¹)(CH₃OH)]·ClO₄ (**1**), a six coordinate oxovanadium(V) complex possessing {VO₄N₂}⁺ coordination environment. The VO³⁺ is coordinated by four donor atoms (ONNO) of di-negative tetradentate (L¹)^{2−} ligand in one plane (the equatorial plane of the octahedron) and favors to form mononuclear oxovanadium(V) complex with octahedral geometry where the sixth position of octahedra is coordinated by CH₃OH molecule instead of ClO₄[−] anion, because lowering of steric crowding with equatorially coordinated tetradentate ligand. While the tetradentate Schiffbase ligand (R,R)-N,N-di-salicylidene cyclohexane 1,2-diamine (H₂L¹) is partially hydrolyzed [29] at pH 7 by VO²⁺ species of VOSO₄ to form tridentate HL² ligand via oxidation of VO²⁺ species to VO³⁺ which then forms oxovanadium(V) moiety of VO₃N₂ coordination environment with tridentate (L²)[−] ligand and the two dioxovanadium(V) moieties are bridged by two oxide ligands to form dimeric oxo-bridged complex [(VO₂L²)₂] (**2**). The schematic representation of the two reactions for the synthesis of **1** and **2** is shown below (Schemes 1 and 2).

3.2. General characterizations, infra-red and electronic spectroscopic studies

The compound **1** in acetonitrile solution shows the molar conductance value of 118 ohm^{−1} cm² mol^{−1} that value can be rationalized by assuming 1:1 electrolyte where the complex is of the composition [VO(HOCH₃)(L¹)]·ClO₄ but compound **2** is non electrolyte in acetonitrile. In compound **1** and **2**, the vanadium ion exists in +5 oxidation state (d⁰ system) and therefore magnetic susceptibility measurement data indicate, both **1** and **2** are diamagnetic at



Scheme 1. Formation of compound **1** from the reaction of H_2L^1 and VO_4^{3-} .



Scheme 2. Probable formation mechanism of compound **2** from the reaction of H_2L^1 and VO^{2+} ion in neutral medium.

298 K. As shown in the experimental section the $\nu(V=O)$ vibrations in **1** (Fig. S1) and **2** (Fig. S2) appears at 974 cm^{-1} and 979 cm^{-1} respectively indicating the ligand effect on $V=O$ vibrations varies in the order of $2 > 1$. The $\nu(C=N)$ of H_2L^1 is observed at 1627 cm^{-1} while in compound **1**, the $\nu(C=N)$ absorption band decreases to 1613 cm^{-1} after chelation with the vanadium center. In case of compound **2**, the $\nu(C=N)$ absorption band for the ligand HL^2 is observed at 1628 cm^{-1} while in compound **2** the $\nu(C=N)$ absorption band is observed at 1614 cm^{-1} which can be rationalized by assuming that the drainage of electron density from nitrogen to vanadium(V) after coordination decreases the π -overlap of C–N bond. The strong C–O(phenolic) vibration band at 1279 cm^{-1} for the free H_2L^1 ligand is shifted to higher energy region ($\nu(C-O_{\text{phenolate}})$ at 1305 cm^{-1}) in compound **1** due to deprotonation of phenolic group increases the C–O bond order by back donation though it is coordinated with the metal ion.

The blue color acetonitrile solution of compound **1** exhibits LMCT transition at wave length 567 nm ($\epsilon = 1800\text{ M}^{-1}\text{ cm}^{-1}$) with two shoulders at 466 and 235 nm . The intra-ligand $\pi \rightarrow \pi^*$ transition is observed at the wave length 249 nm ($\epsilon = 27\,100\text{ M}^{-1}\text{ cm}^{-1}$). While the compound **2** in chloroform solution exhibits a LMCT transition at the wave length 592 nm ($\epsilon = 5300\text{ M}^{-1}\text{ cm}^{-1}$) and an intra-ligand $\pi \rightarrow \pi^*$ transition of aromatic ring at 280 nm ($\epsilon = 99\,100\text{ M}^{-1}\text{ cm}^{-1}$) with two shoulders at 366 and 267 nm .

3.3. Molecular structure of **1** and **2**

The crystal structure of compound **1** revealed by X-ray crystallographic determination showed that the molecular structure of **1** contains discrete $[VO(MeOH)L^1]^+$ cations and perchlorate anions. The geometry of the complex cation $[VO(MeOH)L^1]^+$ shown in Fig. 2 is described as six coordinated octahedral environment of

the metal center where the VO^{3+} ion is bonded to the tetradentate ligand (L^1) $^{2-}$, (N,N-bis(salicylidene)-1,2-diaminocyclohexane) with the oxo ligand O(1) and CH_3OH molecule occupying the axial position of slightly distorted octahedron. The selected bond distances and angles in central metal coordination were listed in Table 3. The vanadium center being displaced above the mean equatorial plane defined by four donor atoms O(64), N(56), N(49) and O(41) of (L^1) $^{2-}$ ligand towards the terminal O(1) by 0.29 \AA with an r.m.s. deviation of 0.04 \AA . The extent of deviation is nearly same for typical monomeric oxovanadium(V) complexes (0.27 – 0.32 \AA) [33,34]. The V1–O1 bond length (1.581 \AA) in $[VO(MeOH)L^1]^+$ lies in the range observed for typical oxovanadium(V) complexes (1.57 – 1.59 \AA) [35]. The longer axial V(1)–O(101) bond length $2.328(3)\text{ \AA}$ indicates that O(101) is being shared by coordinated CH_3OH molecule instead of methoxy anion (CH_3O^-). The molecular packing in **1** show that the oxo groups of two vanadium centers are closely spaced and the perchlorate ions are present in the vicinity of methanol coordinated to vanadium centers indicating the presence of weak interaction between perchlorate ions and methanol (Fig. 3).

The crystal structure of compound **2** revealed by X-ray crystallographic determination showed that the molecule consists of two $[VO_2L^2]$ units (Fig. 4) making it a dimeric centrosymmetric structure (Fig. 5) with two six coordinated octahedral environment. The selected bond distances and angles in central metal coordination were listed in Table 4. There is a striking difference in the two metal–oxygen bond distances of the two bridging oxygen of compound **2** which is formed through asymmetric bridging of two $[VO_2L^2]$ unit.

The V1–O2 bond distance is 1.669 \AA and the O2 bridges to the V1a ($-x, 1-y, 1-z$) at the distance $2.303(3)\text{ \AA}$. Similarly the O2a linked with V1a (V1a–O2a distance is 1.669 \AA) bridges to V1

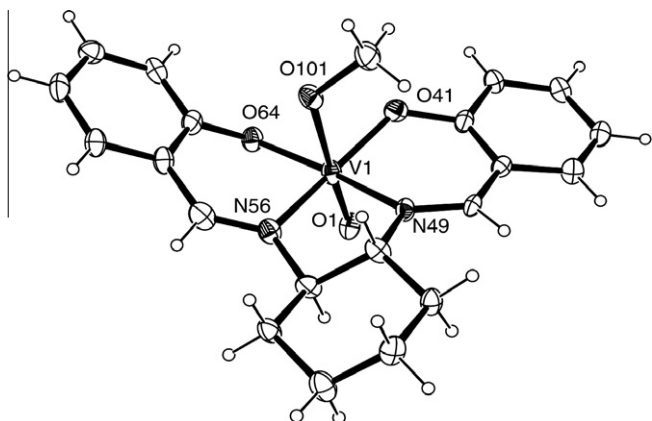


Fig. 2. The structure of $[\text{VO}(\text{MeOH})\text{L}^1]^+$ in **1** with ellipsoids at 25% probability.

at the distance 2.303(3) Å. The vanadium atom(V1) is six coordinated octahedral geometry (Fig. 5) formed by three donor atoms O11, N19, N26 from the planner uni-negative tridentate chiral Schiffbase ligand, (R,R) N-salicylidene cyclohexane 1,2-diamine (HL^2) and two oxo-oxygens O1, O2 and a bridging oxygen O2a. The same octahedral geometry is occurred in the case of other vanadium (V1a). The equatorial plane consist the donor atoms O11, N19, N26 and O2 in case of V1 centered octahedral geometry. In the dimer the two chiral carbons of the ligand (L^1) linked with V1 are C24, C25 possess configuration (R,R) while C24a, C25a of the ligand linked with V1a have the configuration (S,S). A pair of strong hydrogen bonds (N26–H26b...O11a) and (N26a–H26b...O11) of distance 2.169 Å in **2** stabilizes the tight

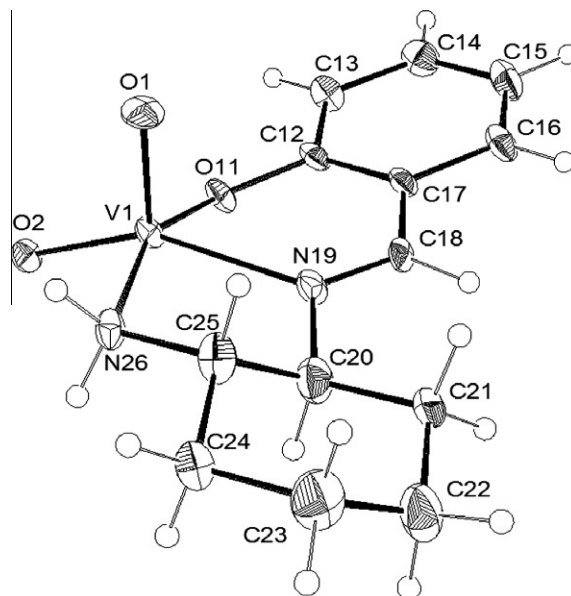


Fig. 4. Square-pyramidal asymmetric unit of dioxovanadium (V), $[\text{VO}_2\text{L}^1]$ of **2**.

dimerization of two $[\text{VO}_2\text{L}^2]$ unit. Therefore observed $\text{V}(1)\cdots\text{V}(1)$ distance (3.108(1) Å) and $\text{V1}-\text{O2a}$ (2.303(3) Å) are the shortest distances than the earlier reported di-(μ-oxo) bridged vanadium(V) complex $[\text{V}_2\text{O}_4\text{L}_2]$ [36,37] (where L is any uni-negative tridentate ligand). The apical oxo-vanadium $\text{V1}-\text{O1}$ double bond distance is 1.608(4) [38]. The $\text{V1}-\text{O2}$ bond distance 1.669 Å which is slightly larger than the $\text{V1}-\text{O1}$ double bond (1.608 Å) and smaller the $\text{V1}-\text{O11}$ single bond (1.91 Å) due to delocalization of $\pi(\text{pi})$ electrons of O2 atom by asymmetric oxo bridging of the two penta-coordinated $[\text{VO}_2\text{L}^2]$ units the $\text{V1}-\text{O2}$ double bond nature is reduced. The molecular packing in **2** exhibits two different kinds of hydrogen bonding networks (Fig. 6 and Table 5). In **2**, a pair of intra-molecular $\text{N26}-\text{H}(26\text{b})\cdots\text{O11}$ hydrogen bonds stabilize the dimeric form via tight dimerization of two asymmetric VO_2L^1 unit forming two $\text{R}_1^1(6)$ ring. The other two weak intermolecular

Table 3
Selected bond lengths (Å) and angles (°) for complex **1**.

$\text{V}(1)-\text{O}(1)$	1.581(2)	$\text{O}(1)-\text{V}(1)-\text{O}(64)$	103.34(12)
$\text{V}(1)-\text{O}(41)$	1.849(2)	$\text{O}(1)-\text{V}(1)-\text{O}(41)$	99.68(12)
$\text{V}(1)-\text{O}(64)$	1.828(3)	$\text{O}(64)-\text{V}(1)-\text{O}(41)$	104.72(12)
$\text{V}(1)-\text{O}(101)$	2.328(3)	$\text{O}(1)-\text{V}(1)-\text{N}(49)$	91.51(12)
$\text{V}(1)-\text{N}(49)$	2.096(3)	$\text{O}(64)-\text{V}(1)-\text{N}(49)$	159.51(12)
$\text{V}(1)-\text{N}(56)$	2.099(3)	$\text{O}(41)-\text{V}(1)-\text{N}(49)$	86.25(12)
$\text{O}(1)-\text{V}(1)-\text{N}(56)$	98.37(13)	$\text{O}(1)-\text{V}(1)-\text{O}(101)$	171.96(12)
$\text{O}(64)-\text{V}(1)-\text{N}(56)$	87.04(13)	$\text{O}(64)-\text{V}(1)-\text{O}(101)$	83.70(10)
$\text{O}(41)-\text{V}(1)-\text{N}(56)$	155.45(11)	$\text{O}(41)-\text{V}(1)-\text{O}(101)$	82.02(10)
$\text{N}(49)-\text{V}(1)-\text{N}(56)$	76.77(13)	$\text{N}(49)-\text{V}(1)-\text{O}(101)$	80.73(10)

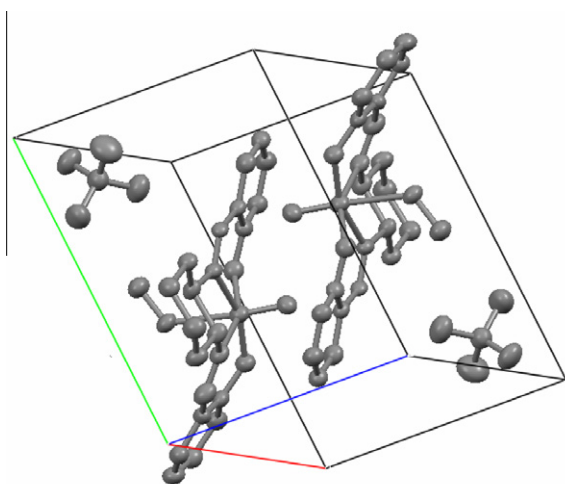


Fig. 3. The molecular packing in the complex $[\text{VO}(\text{MeOH})\text{L}^1]\cdot\text{ClO}_4$, **1**.

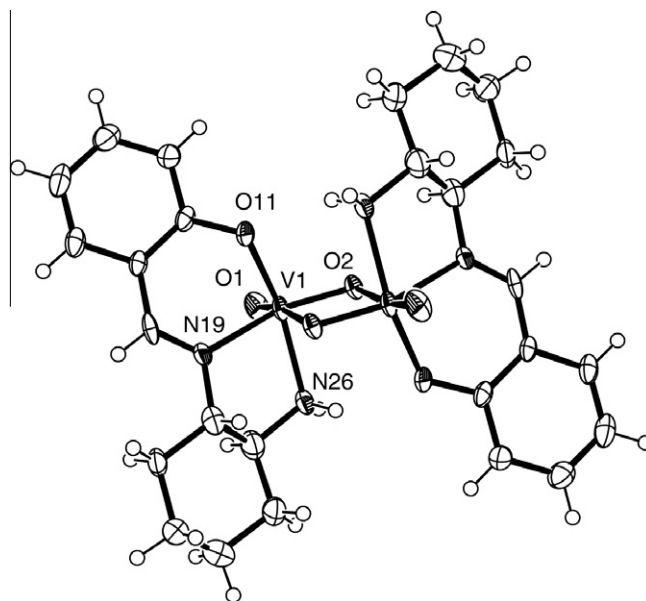


Fig. 5. The centrosymmetric structure of **2** ($[\text{VO}_2\text{L}^2]_2$) together with the atomic numbering scheme, ellipsoids at 25% probability.

Table 4
Selected bond lengths (Å) and angles (°) for complex **2**.

V(1)–N(19)	2.147(4)	O(11)–V(1)–N(26)	158.06(17)
V(1)–O(1)	1.608(4)	O(11)–V(1)–N(19)	85.02(16)
V(1)–O(11)	1.912(4)	N(26)–V(1)–N(19)	76.81(16)
V(1)–N(26)	2.114(4)	O(11)–V(1)–O(2)\$1	84.26(14)
V(1)–O(2)	1.669(3)	N(26)–V(1)–O(2)\$1	79.29(15)
V(1)–O(2)\$1	2.303(3)	N(19)–V(1)–O(2)\$1	75.06(15)
O(1)–V(1)–O(2)	106.25(19)	V(1)–O(2)–V(1)\$1	101.77(16)
O(1)–V(1)–O(11)	101.44(18)	O(1)–V(1)–N(19)	99.51(18)
O(2)–V(1)–O(11)	99.21(16)	O(2)–V(1)–N(19)	152.39(17)
O(1)–V(1)–N(26)	93.69(19)	O(1)–V(1)–O(2)\$1	171.88(18)
O(2)–V(1)–N(26)	91.58(17)	O(2)–V(1)–O(2)\$1	78.23(16)

\$1 Symmetry element $-x, 1-y, 1-z$.

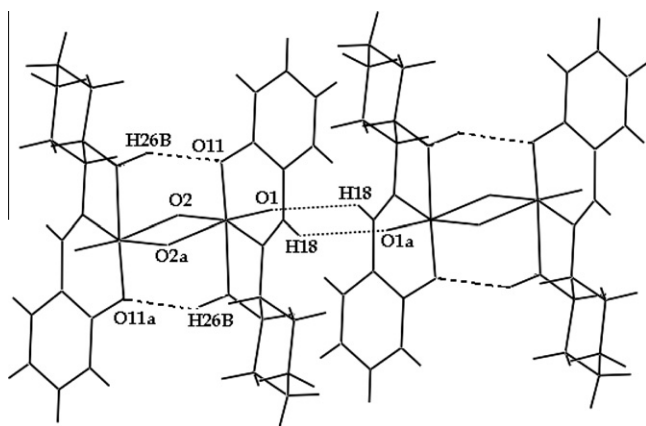
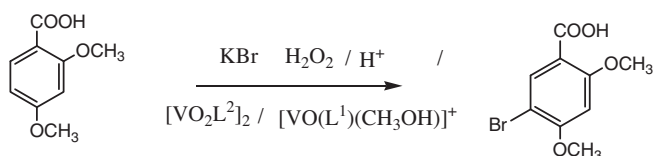


Fig. 6. The intra- and inter-molecular H-bonded (N–H···O and C–H···O) figure of $[(VO_2L^2)_2]$ (**2**) with the direction of the cell axes is (1 0 0).

Table 5
Relevant hydrogen bonds for complex **2**.

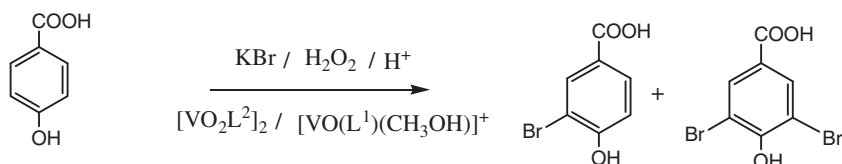
D–H···A	d(D–H)	d(H···A)	d(D···A)	∠(DHA)
N(26)–H(26B)···O(11) ⁽ⁱ⁾	0.90	2.17	2.968(6)	147
C(18)–H(18)···O(2) ⁽ⁱⁱ⁾	0.93	2.37	3.205(6)	150
C(21)–H(21B)···O(2)	0.97	2.59	3.468(7)	151

Symmetry codes: (i) $-x, 1-y, 1-z$ (ii) $1/2-x, 1/2+y, 1-z$.

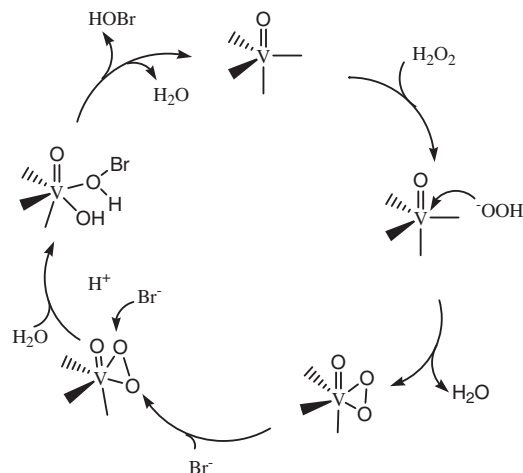


Scheme 3. Catalytic bromination of 2,4-dimethoxy benzoic acid using **1** and **2** as catalyst.

hydrogen bonding interaction C(18)–H(18)···O(2) and C(21)–H(21B)···O(2) (Fig. 6) in **2** produced infinite one-dimensional chain propagating along the (1 0 0) direction.



Scheme 4. Catalytic bromination of p-hydroxy benzoic acid using **1** and **2** as catalyst.



Scheme 5. Probable mechanism of bromide oxidation by oxovanadium(V) complex [39] in presence of KBr and H_2O_2 .

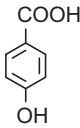
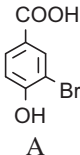
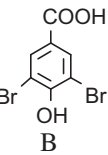
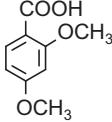
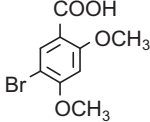
3.4. Catalytic bromination of aromatic compounds

In presence of hydrogen peroxide, both the monomeric and dimeric oxovanadium(V) complex **1** and **2** respectively forms oxoperoxo-vanadium(V) species which subsequently oxidizes the bromide ion in acidic condition (pH 3–4) as catalyst to form Br^+ (exists as Br_3^- , Br_2 or $HOBr$) (shown in Scheme 5) [39]. Thus, the in situ generated bromonium species leads to formation of brominated organic products by reacting with suitable organic substrates. It has been seen that in presence of very low pH (<1), the suitable organic compounds are brominated by H_2O_2/Br^- to a very small amount and at pH >3 the yields of brominated products are very poor after a long period of reaction. Such as, the organic compounds 4-hydroxy benzoic acid and 2,4-dimethoxy benzoic acid are not brominated effectively (2–5% after 10 h reaction) by H_2O_2/Br^- system in acidic condition (pH 3–4) in the absence of the catalyst, but in presence of catalyst (**1** or **2**) both 4-hydroxy benzoic acid (Scheme 3) and 2,4-dimethoxy benzoic acid (Scheme 4) yield 98% brominated products after 12 h of reaction period. The reactions are shown in the Schemes 4 and 5. The catalytic efficiency of compound **1** is slightly higher compared to that of compound **2** may be (Table 6) due to the high stability of the dimeric form of **2** that inhibits peroxidic attack to the metal center. The solid brominated products are characterized by 1H NMR spectra.

3.5. Characterizations of brominated products by 1H NMR spectroscopic studies

In the substrate molecule, 2,4-dimethoxy benzoic acid, the chemical shifts for ortho- and para-methoxy hydrogen are observed at δ 3.88 (s, 3H) and 4.04 (s, 3H) respectively. Chemical shifts for three single H atom attached with C3, C5 and C6 carbon atoms of aromatic ring observed at δ 6.53 (s, 1H), 6.63 (d, 1H, $J = 10.5$ Hz) and 8.12 (d, 1H, $J = 8.64$ Hz) respectively (Fig. S3) while in the mono brominated (5-bromo 2,4-dimethoxy benzoic acid) product,

Table 6
Details of the catalytic bromination by compound **1** and **2** used as catalyst in presence of KBr and H₂O₂ in acid medium and CH₃CN is used as solvent. Substrate:catalyst = 1000:1.

Entry	Substrate	Product/s	Time (h)	% Yields (mmol) for catalyst		% Selectivity/proportion for catalyst		Turn over number (TON)	
				1	2	1	2	1	2
I		 A  B	15	85	68	A-67 B-33	A-69 B-31	850	680
II			12	98	78	100	100	980	780

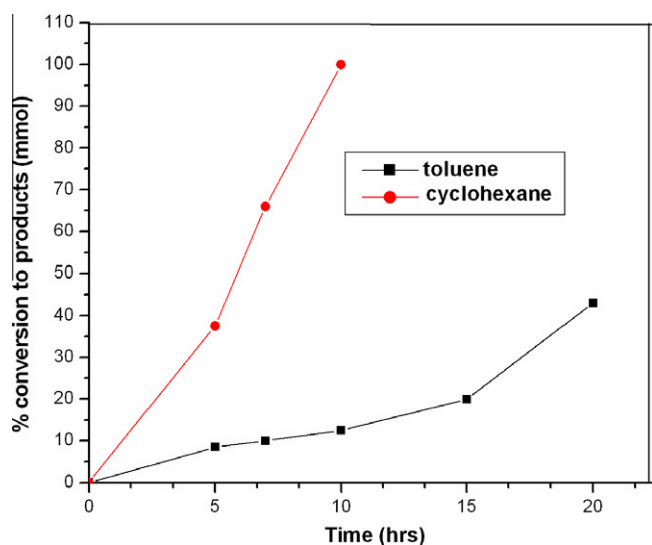


Fig. 7. The plot of products percentage with time for the catalytic oxidation of toluene and cyclohexane.

the chemical shifts of the two methoxy group are obtained at δ 3.99 (s, 3H) and 4.09 (s, 3H). Another two singlets for two aromatic protons are observed at δ 6.51 (s, 1H) and 8.33 (s, 1H) which are shown in the figure (Fig. S4). In the case of the substrate, para-hydroxy benzoic acid, the chemical shifts for two ortho hydrogen atoms is observed at δ 7.32 (d, 2H, J = 8.86 Hz) and for two meta hydrogen at δ 6.73 (d, 2H, J = 8.67 Hz) respectively. The chemical shift for –OH hydrogen is observed at δ 5.30 (s, 1H). In mono brominated products (3-bromo 4-hydroxy benzoic acid), the chemical shifts are observed at δ 5.30 (s, 1H for –OH group), 6.90 (d, 1H, J = 8.62 Hz for meta- H of aromatic ring), 7.32 (d, 1H, J = 8.85 Hz for one ortho(6-) H atom) and 7.77 (s, 1H of another ortho(2-) H atom) respectively (Fig. S5). In the dibrominated (3,5-dibromo 4-hydroxy benzoic acid) only two singlets are observed in the ¹H NMR spectrum (Fig. S6) and chemical shifts for these two are at δ 7.769 (s, 2H of two ortho aromatic H atoms) and 5.30 (s, 1H), respectively. The magnitude of the NMR signal in the mixture of products indicates that mono brominated is the major product.

3.6. Catalytic oxidation of hydrocarbons

Complexes **1** and **2** possess effective catalytic properties in the oxofunctionalization of representative hydrocarbons cyclohexane,

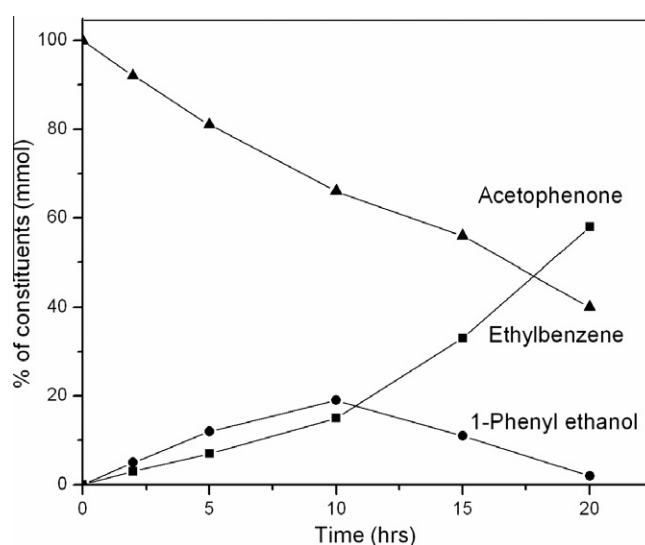


Fig. 8. The proportion diagram of products and substrate during the course of catalytic oxidation in case of ethylbenzene.

ethyl benzene and toluene to their alcoholic and carbonyl functions as shown in the Table 2. The catalytic efficiency of the two oxovanadium(V) complexes **1** and **2** for hydrocarbon oxidation are not same (shown in the Table 2) due to their different coordination geometry probably because of the tight dimerisation of two oxovanadium(V) nucleus in complex **2** which makes it less reactive towards H₂O₂ activation. After 10 h cyclohexane is totally oxidized (Fig. 7) to cyclohexanol and cyclohexanone with high turnover number (TON), while toluene is selectively oxidized to benzaldehyde (43%) after the period of 20 h without any side products (Fig. 7). In case of ethyl benzene, the C–H bonds of benzyl carbon are easily oxidized to form acetophenone (58%) as major products (Fig. 8) instead of 1-phenyl ethanol (2%) up to a reaction period of 20 h. The lower yield of toluene oxidation compared to ethylbenzene indicates that the C–H bond of secondary carbon is more labile towards oxidation rather than that with primary carbon. However, the Fig. 9 indicates that the cyclohexanol (oxidized product of cyclohexane) is further oxidized to cyclohexanone by the same catalyst in the reaction medium. So, during the course of reaction, the proportion of cyclohexanone is increased with a higher degree than cyclohexanol. The mechanism of the peroxidative hydrocarbon oxidation by oxovanadium(V) based catalyst is same as appeared in our previous work [40].

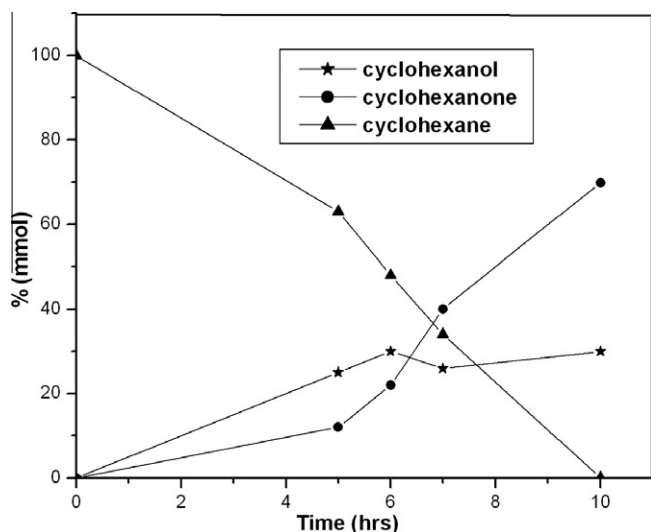


Fig. 9. The proportion diagram of products and substrate during the course of catalytic oxidation in case of cyclohexane.

4. Conclusions

The potentiality of both the monomeric and dimeric chiral Schiffbase complexes attached to VO^{3+} and VO_2^+ moiety, respectively, is very high. When compared between them, the monomer possesses high potentiality in relation to the peroxidative bromination and hydrocarbon oxidation than that of the dimer. So far as our knowledge goes herein the very high turnover of peroxidative bromination of the aromatic compounds by using the model complex is reported.

Acknowledgements

The authors are very much thankful to Late Prof. Ramgopal Bhattacharyya for of his cooperation, encouragement, and constructive suggestions. T.K.S. thanks CSIR (Award No. 9/96(0624) 2K10-EMRI dated 10.03.2010) for Research Associateship. Funding by DST, INDIA for Agilent 6890N Gas Chromatograph with dual detector facilities and EPSRC and the University of Reading for the X-Calibur system are thankfully acknowledged.

Appendix A. Supplementary data

CCDC 805362 and 805363 contains the supplementary crystallographic data for compound **1** and **2**. These data can be obtained free of charge via <http://www.ccdc.cam.ac.uk/conts/retrieving.html>, or from the Cambridge Crystallographic Data Centre, 12 Union Road, Cambridge CB2 1EZ, UK; fax: (+44) 1223-336-033; or e-mail: deposit@ccdc.cam.ac.uk. The figures of IR spectra (Figs. S1 and S2) and ^1H NMR spectra (Figs. S3–S6) are available in the supplementary file. Supplementary data associated with this article can be found, in the online version, at doi:10.1016/j.poly.2011.06.005.

References

- [1] A.E. Shilov, G.B. Shul'pin, Russ. Chem. Rev. 59 (1990) 853.
- [2] (a) S.T. Oyama, J.W. Hightower (Eds.), Catalytic Selective Oxidation, American Chemical Society, Washington, 1993;

- (b) H. Mimoun, L. Saussine, E. doire, M. Postel, J. Fischer, R. Weiss, J. Am. Chem. Soc. 105 (1983) 3101.
- [3] First search in 1984, see H. Vilter, Phytochemistry 23 (1984) 1387.
- [4] (a) I.G. Fantus, J. Kadota, G. Pergon, B. Foster, B.I. Posner, Biochemistry 28 (1989) 8864;
- (b) C. Slebodnick, B.J. Hamstra, V.L. Pecoraro, Struct. Bond. (Berlin) 89 (1997) 51.
- [5] (a) D. Rehder, Coord. Chem. Rev. 182 (1999) 297;
- (b) A. Butler, J.V. Walker, Chem. Rev. 93 (1993) 1937;
- (c) A. Butler, in: K. Redjik, E. Bouwman (Eds.), Bioinorganic Catalysis, second ed., Marcel Dekker, New York, 1999.
- [6] (a) C. Slebodnick, N.A. Law, V.L. Pecoraro, in: B. Mernier (Ed.), Biomimetic Oxidation Catalyzed by Transition Metal Complexes, Imperial College Press, London, 2000;
- (b) H. Vilter, in: H. Sigel, A. Sigel (Eds.), Metal Ions in Biological Systems: Vanadium and its Role in Life, vol. 31, Marcel Dekker, New York, 1995.
- [7] (a) R.A. Carter-Franklin, R.D. Little, A. Butler, J. Am. Chem. Soc. 125 (2003) 3688;
- (b) K.-H. Van pee, S. Keller, T. Wage, L. Wynads, H. Schnerr, S. Zehner, Biol. Chem. 381 (2000) 1;
- (c) A. Butler, Coord. Chem. Rev. 187 (1999) 17.
- [8] A. Butler, Science 281 (1998) 207.
- [9] H.S. Soedijk, A. Butler, Inorg. Chem. 29 (1990) 5015.
- [10] (a) R. Wever, H. Plat, E. de Boer, Biochem. Biophys. Acta 830 (1985) 181;
- (b) R.R. Everett, H.S. Soedijk, A. Butler, J. Biol. Chem. 265 (1990) 15671.
- [11] S. Tanaka, H. Yamamoto, H. Nozaki, K.B. Sharpless, J. Am. Chem. Soc. 96 (1974) 5254.
- [12] Y. Hoshino, H. Yamamoto, J. Am. Chem. Soc. 122 (2000) 10452.
- [13] C. Bolm, T. Kühn, Synlett (2000) 899.
- [14] W. Adam, A.K. Beck, A. Pichota, C.R. Saha-Moller, D. Seebach, N. Vogl, R. Zhang, Tetrahedron Asymmetry 14 (2003) 1355.
- [15] A. Lattanzi, S. Picirillo, A. Scettri, Eur. J. Org. Chem. (2005) 1669.
- [16] M. Bonchio, V. Conte, F. Di Furia, G. Modena, J. Org. Chem. 54 (1989) 4368, and references cited therein.
- [17] M. Bonchio, V. Conte, F. Di Furia, G. Modena, J. Org. Chem. 59 (1994) 6262.
- [18] A. Butler, J. Clause, G.E. Meister, Chem. Rev. 94 (1994) 625.
- [19] (a) T.K. Si, K. Chowdhury, M. Mukherjee, D.C. Bera, R. Bhattacharyya, J. Mol. Catal. A Chem. 219 (2004) 241;
- (b) H.H. Monfared, S. Kheirabadia, N.A. Lalami, P. Mayer, Polyhedron 30 (2011) 1375.
- [20] D.A. Cogan, G. Liu, K. Kim, B.J. Backes, J.A. Ellman, J. Am. Chem. Soc. 120 (1998) 8011.
- [21] H.B. tenBrink, A. Tuynman, H.L. Dekker, W. Hemrika, Y. Izumi, T. Oshiro, H.E. Shoemaker, R. Wever, Inorg. Chem. 37 (1998) 6780.
- [22] G. Du, H.J. Esperson, Inorg. Chem. 44 (2005) 2465.
- [23] (a) F.A. Cotton, G. Wilkinson (Eds.), Advanced Inorganic Chemistry, fifth ed., Wiley, New York, 1988, p. 673;
- (b) A. Sarkar, S. Pal, Polyhedron 25 (2006) 1689, and references cited there in;
- (c) K. Oyaizu, E.L. Dewi, E. Tsuchida, Inorg. Chem. 42 (2003) 1070.
- [24] D.C. Crans, J.J. Smee, E. Gaidamauskas, L. Yang, Chem. Rev. 104 (2004) 849.
- [25] S. Mohebbi, A.H. Sererstini, Transition Met. Chem. 32 (2006) 749.
- [26] K. Nakajima, K. Kojima, K. Toriumi, K. Saito, J. Fujita, Bull. Chem. Soc. Jpn. 62 (1989) 760.
- [27] (a) H. Schmidt, M. Bashirpoor, D. Rehder, J. Chem. Soc., Dalton Trans. (1996) 3865;
- (b) D. del Río, A. Galindo, R. Vicente, C. Mealli, A. Ienco, D. Masi, Dalton Trans. (2003) 1813.
- [28] (a) M. Kojima, H. Taguchi, M. Tsuchimoto, K. Nakajima, Coord. Chem. Rev. 237 (2003) 183;
- (b) S. Liang, D.V. Derveer, S.Y. Qian, B. Sturgeon, X.R. Bu, Polyhedron 21 (2002) 2021.
- [29] F. Aveçilla, P. Adão, I. Correia, J.C. Pessoa, Pure Appl. Chem. 81 (2009) 1297.
- [30] CRYSLIS, Oxford Diffraction Ltd., Version 1, 2005.
- [31] G.M. Sheldrick, Shelx97, Program for Crystal Structure Calculations, University of Gottingen, 1997.
- [32] ABSPACK, Oxford Diffraction Ltd., 2005.
- [33] L. Banci, A. Bencini, A. Dei, D. Gatteschi, Inorg. Chim. Acta 84 (1984) L11.
- [34] E. Tsuchida, K. Oyaizu, Coord. Chem. Rev. 237 (2003) 213.
- [35] D. Rehder, M. Ebel, C. Wikete, G. Santoni, J. Gätjens, Pure Appl. Chem. 77 (2005) 1607.
- [36] X. Li, M.S. Lah, V.L. Pecoraro, Inorg. Chem. 27 (1988) 4657.
- [37] C.A. Root, J.D. Hoeschele, C.R. Cornman, J.W. Kampf, V.L. Pecoraro, Inorg. Chem. 32 (1993) 3855.
- [38] J.A. Bonadies, W.M. Butler, V.L. Pecoraro, C.J. Carrano, Inorg. Chem. 26 (1987) 1218.
- [39] M.R. Maurya, S. Agarwal, C. Bader, M. Ebel, D. Rehder, Dalton Trans. (2005) 537.
- [40] T.K. Si, S. Chakraborty, A.K. Mukherjee, M.G.B. Drew, R. Bhattacharyya, Polyhedron 27 (2008) 2233.